JOURNAL OF OPTOELECTRONICS AND ADVANCED MATERIALS Vol. 10, No. 10, October 2008, p. 2607 - 2610

Structural and photoluminescence properties of $Zn_{1-x}Mn_xO$ nanoparticles for optoelectronic device applications

D. SREEKANTHA REDDY[a], S. K. SHARMA[b], Y. D. REDDY[c], B. S. REDDY[c], K. R. GUNASEKHAR[b], P. SREEDHARA REDDY[c]

[a]*Department of Physics, Chungbuk National University, Cheongju 361-763, Republic of Korea*
[b]*Department of Instrumentation, Indian Institute of Science, Bangalore-560012, India*
[c]*Department of Physics, Sri Venkateswara University, Tirupati-517502, India*

High intense photoluminescence $Zn_{1-x}Mn_xO$ powder samples were prepared by simple solid state reaction method. All the samples were studied for their morphological, structural and photoluminescence properties. X-ray diffraction (XRD) results showed that all the samples were polycrystalline with wurtzite structure. The lattice parameters 'a' and 'c' varied linearly with composition following Vegard's law in this composition range. Scanning Electron Microscopy (SEM) studies showed that all the samples investigated were in nanoparticles form with the particle size lying in the range 25 – 50 nm. The room temperature photoluminescence spectra show that the UV emission gradually shifted towards the higher energy side. A blue-shift in the position along with an intense blue emission band was observed with the Mn concentrations, which are ascribed to the quantum confinement effect.

(Received March 12, 2008; accepted August 14, 2008)

Keywords: Diluted Magnetic semiconductors; Optoelectronics; Nanoparticles; Photoluminescence.

1. Introduction

During the last few decades, ZnO based diluted magnetic semiconductors have gained interest, because of the interesting and important properties of ZnO such as wide direct band gap of 3.37 eV [1] at room temperature. Consequently, ZnO becomes one of the materials that have got encouraging potential as blue ultraviolet light emitters and detectors, transparent high power electronics and piezoelectric transducers. Its low threshold for optical pumping and large exciton binding energy (60 meV) [2, 3] allow lasing action in ZnO to be reached at extremely low pumping power at room temperature [4] being recognized as a promising photonic material in the UV region [5]. Mn doped ZnO samples have nonlinear variation of the band gap with composition is observed [6]. The deviation from linearity could lead to the presence of a minimum band gap. Thus, the absorption, photoconductivity and photoluminescence (PL) spectra provide basic information for understanding optical progress in DMS materials [7]. The DMS shows a variety of marked magneto-optical properties due to the exchange interaction of the band electrons with the magnetic ions.

The luminescence due to the transition $^4T_1(G)\rightarrow{}^6A_1(S)$ of Mn^{2+} in II-VI compounds can be excited directly by absorption within the 3d shell by excitation of the other impurities or of the lattice respectively, followed by an energy transfer [8]. Several energy transfer mechanism have been discussed [9]. In the past few decades, DMS of $A^{II}_{(1-x)}Mn_xB^{VI}$ type alloys (where A^{II} = Zn, Cd, Hg and B^{VI} = S, Se, Te,) have been studied [10 - 11]. Numerous reports have been devoted to either semiconducting or photoluminescence or magnetic properties of selenides, tellurides and sulphides only. However, the luminescence studies on ZnO based DMS are very few. In view of this, we have planed to investigate the ZnO based DMS to optimize its preparation conditions for suitable applications. The resulting $Zn_{1-x}Mn_xO$ samples were characterized in terms of surface morphology, structural and photoluminescence properties.

2. Experimental procedure

High photoluminescence intensity $Zn_{1-x}Mn_xO$ powder samples with x = 0, 0.02 and 0.04 were prepared by simple inexpensive solid state reaction method. A quartz tube with provision to allow unwanted vapours to escape from the reaction chamber and which could be evacuated and isolated was designed and was used for synthesis of the present samples. Appropriate quantities of 5N pure ZnS and MnO powders (Sigma Aldrich, Germany) were thoroughly mixed by grinding them with pestle and mortar. After that these was loaded into a one end closed quartz tube of 10 mm diameter and 8 cm long. The other end was plugged with quartz wool. The quartz tube was inserted into the synthesizer and fired for several hours at different temperatures. The optimum firing temperatures and firing periods to yield intense photo luminescent samples were arrived at after great deals of trial and error procedure were found to be 1273 K and 10 h, respectively. The deposited ZnS films were subjected to various

characterization studies. The grain size was estimated using Scanning electron microscopy (SEM, model: JSM 840A). The structure of the films was studied using powder X-ray diffractometer (XRD) in the scanning range of $2\theta = 20^0 - 70^0$. The photoluminescence properties are studied at room temperature by Fluorolog-3 fluorescence spectrometer.

3. Results and discussion

3.1. Structural analysis

The X-ray diffraction patterns are obtained by Seifert XRD 3003 TT with CuK_α (λ = 1.5406Å) radiation using Ni filter. All measurements were carried out in the scanning range $2\theta = 20^0 - 70^0$.

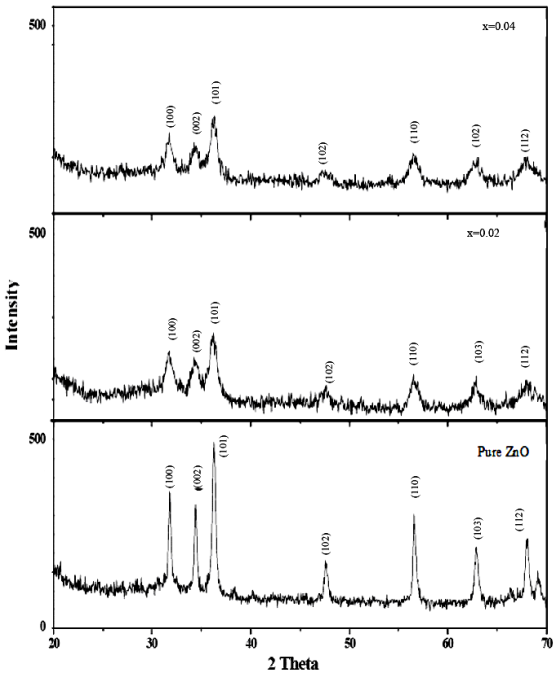

Fig. 1 XRD patterns of $Zn_{1-x}Mn_xO$ powder samples prepared at 1273 K.

Fig. 1 shows the XRD patterns corresponding to $Zn_{1-x}Mn_xO$ powder samples synthesized at different atomic fractions of Mn (x = 0, 2 % and 4 %). X-ray diffraction (XRD) results showed that all the samples were polycrystalline with wurtzite structure. The peak broadening reveals that the samples are in nanocrystalline nature. Using the JCPDS data, the lattice parameters 'a', 'c' and also the volume of the cell have been calculated. The lattice parameters 'a' and 'c' were varied with the increase of Mn content is shown in Fig. 2 that follows the Vegard's law. The variation of volume of the unit cell with respect to the Mn content has shown in Fig. 3. These variations occur due to the difference of Mn^{2+} ionic radius with the Zn^{2+} ionic radius. Both 'a' and 'c' axis lengths varied monotonically with the increase of Mn content. The valance state of Mn ion is determined to be Mn^{2+} having spin 5/2 for electronic spin resonance measurements [12].

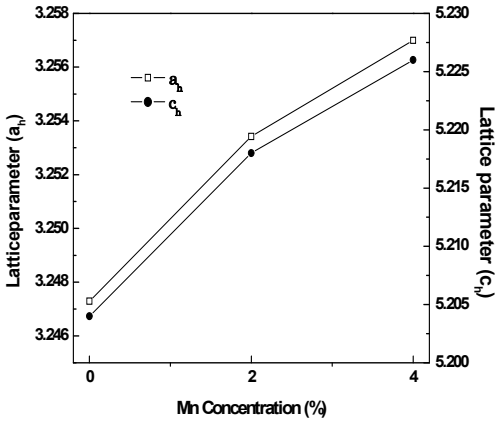

Fig. 2 Variation of lattice parameters 'a' and 'c' with Mn concentration.

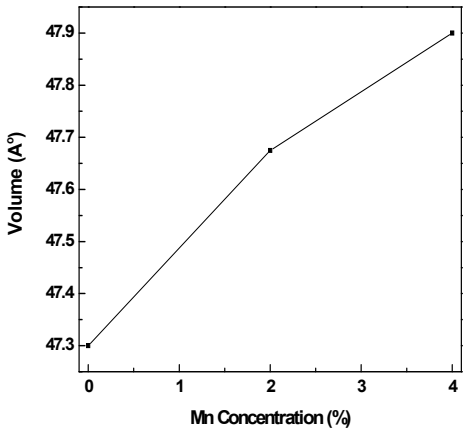

Fig. 3 Variation of cell volume with the Mn concentration.

Therefore, the Mn ion is understood to have occupied the Zn site without changing the crystal structure. The average size of the grain size is calculated by the Debye-Scherrer's formula and the crystallite size of the samples lie from 25 nm to 50 nm.

3.2. Surface morphology studies

The surface morphology of the pure ZnO and 4% Mn doped ZnO exhibits like nanorods and nanoparticles are shown in Fig. 4. It is revealed that the product consists of well-defined rods and particles like morphology composed of multi-nanorods and nanoparticles. The average diameter of the nanorods is about 75-150 nm and average particle size 25-50 nm. The average grain size of these samples, evaluated using a statistical averaging technique, decreased with concentration, and these values nearly match the data obtained from the XRD studies.

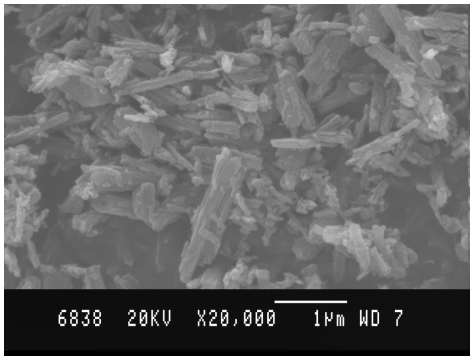

(a)

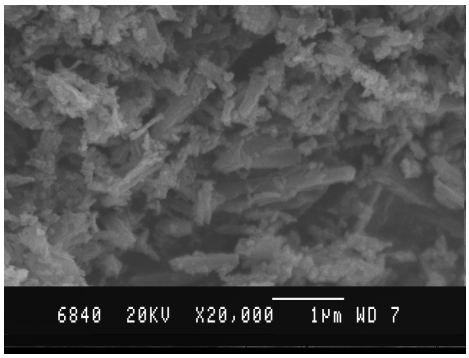

(b)

Fig. 4 SEM images of (a) pure ZnO and (b) $Zn_{0.96}Mn_{0.04}O$ powder samples.

3.3. Photoluminescence studies

Fig. 5 shows the excitation spectra for the pure ZnO at room temperature using emission wavelength at 454 nm and the samples have been prepared at 1273 K. The excitation wavelength used for all samples is 379 nm. By this excitation wavelength, the emission spectra of reference ZnO and Mn doped ZnO samples are analyzed. The broad blue emission band is observed which is shown in Fig. 6.

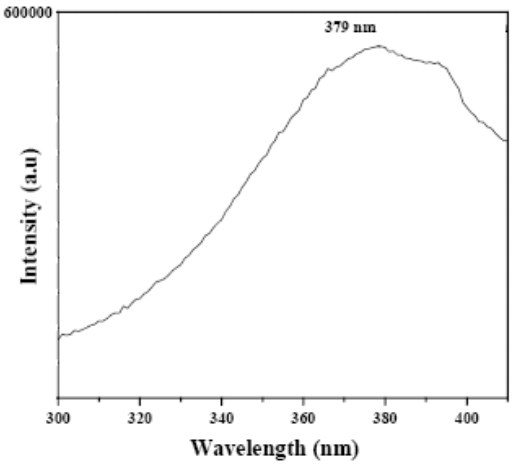

Fig. 5 Excitation spectrum for the pure ZnO powder samples.

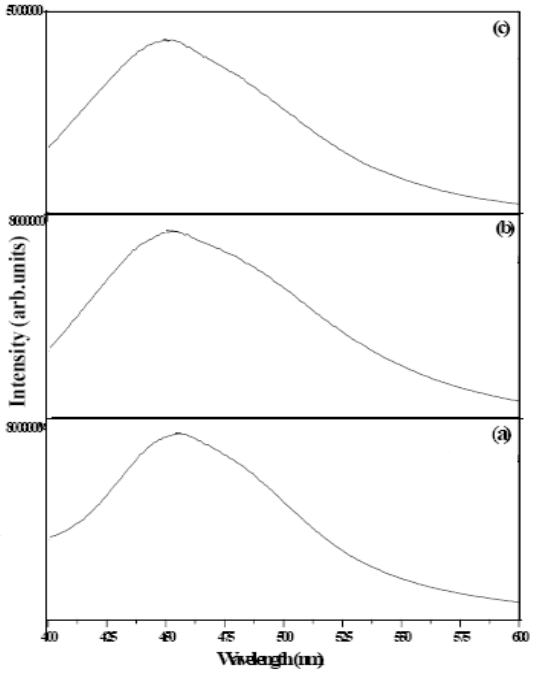

Fig. 6 Emission spectra of $Zn_{1-x}Mn_xO$ powder samples.

In all these systems, the emission bands are not sharp peaks but are broad bands and because of the presence of many recombination sites, the grains have different impurity concentrations, surface areas and defects types. Hence the individual emissions have a range of energies and hence from broad bands. For low concentrations of Mn, maximum photoluminescence intensity has been observed and the intensity decreases together with the broadening of the FWHM (Full Width at Half Maximum) as a function of Mn content. The green luminescence mechanism of ZnO has been studied and various models have been proposed [13 - 16] proved that a single ionized oxygen vacancy is responsible for green emission in the ZnO and the emission results from recombination of a photo-generated hole with an electron occupying the oxygen vacancy. It is generally believed that the blue emissions are due to excitonic transitional defects states, in particular, the oxygen vacancies and Zinc interstitials [17, 18]. The blue emission shifts to a lower wavelength side, that means is shifts towards a higher energy side with an increase of Mn content because of the energy gap of manganese oxide is 4.2 eV which is greater than the Zinc Oxide (3.37 eV). This emission could be due to band exciton extrinsic transitions and are related to dopants or defects or oxygen vacancies and zinc interstitials, which usually create discrete electronic states in the band gap and therefore, which influence both the optical absorption and the emission spectra.

4. Conclusions

The diluted magnetic semiconductor $Zn_{1-x}Mn_xO$ nanopowder samples were prepared simple inexpensive

solid state reaction method. The nanopowders are found to be in hexagonal wurtzite structure and all are in polycrystalline and the broadening in the peaks indicates the nanonature of the samples and the size of the crystallite have been computed by Debye-Scherrer's equation the average crystallite sizes are varied from 25 nm to 50 nm. SEM studies shoes that the average diameter of the nanorods is about 75 - 150 nm and average particle size 25 - 50 nm. The photoluminescence spectra made on the bulk nanopowders show visible blue and green emission, which could be attributed to single ionized oxygen vacancies and zinc interstitials.

References

[1] Y. Ohto, T. Haga and Y. Abe Jpn. J. Appl. Lett **36,** L1040 (1997).
[2] D. C. Look Mater. Sci. Eng., B **80,** 381 (2001).
[3] D. C. Reynolds, D. C. look, B. Jogai, C. W. Litton, G. Gantwell and W. C. Harsch Phys. Rev. B: Concdens. Matter **60**, 2340 (1999).
[4] U. Ozgur, Ya. I. Alivov, C. Liu, A. Teke, M. A. reshcchikov, S. Dogan, V. Avrutin, S. J. Cho and H. Morkoc; J. Appl. Phys **98**, 041301 (2005).
[5] K. J. Ko, Y. F. Chen, T. Yao, I. Kobayashi and H. Uchiki; Appl. Phys. Lett. **76 (11)**, 1905 (2000).
[6] M. Ikeda, K. Ihow, S. Hisano; J. Phys. Soc. Jpn. **25**, 455 (1968).
[7] J. Wedermeyer, U. Stutenbaumer, H. E. Gumlich; J. Lumin **40**, 533 (1988).
[8] T. Hashina, H. Kawai, Jpn. J. Appl. Phys **19**, L267 (1980).
[9] J. Oladeji, L. Chow, J. R. Liu, W. K. Chu, A. N. Dbustamante, C. Fredricken, A. F. Schulte; Thin Solid Films **359**, 154 (2001).
[10] Ozsan, D. R. Johnson, M. Sadegri, P. Sivapathasundaram, G. Good, Let. M. J. Furlong, L. M. Peter, A. A. Shingleton, J. Mater. Sci. Mater. Electronics **7**, 119 (1990).
[11] L. Levi, N. Felton, D. Ingert; J. Phys. Chem B **102**, 9153 (1993).
[12] T. Fukumura, M. Kawasaki, M. Mizuguchi, H. Hosoka Phys. Rev. **112**, 1058 (1958).
[13] F. A. Krogerk, H. J. Vink; J. Chem. Phys. **22**, 250 (1954).
[14] E. G. Bylander, J. Appl. Phys. **49**, 1188 (1978).
[15] J. A. Voigt, B. E. Gnade; J. Appl. Phys. **79**, 7983 (1996).
[16] W. S. Shi, O. Agyeman, C. N. Xu; J. Appl. Phys. **91**, 5640 (2002).
[17] W. S. Mo, M. W. Shao, H. M. Hu, L. Yang, W. C. Yu, Y. T. Qua. J. Crys. Growth **244**, 364 (2002).
[18] J. B. Liang, J. W. Liu, Q. Xie, S. Bai, W. C. Yu, Y. T. Qin; J. Phys. Chem **199**, 9463 (2005).

Corresponding author: dsreddyphd@gmail.com